AD-A148 787 AUTONOMOUS NAVIGATION FOR MOBILE ROBOT VEHICLES OVER HILLY TERRAIN USING.. (U) ARMY ARMAMENT RESEARCH AND DEVELOPMENT CENTER WATERVLIET NY L.. C N SHEN OCT 84 1/1

UNCLASSIFIED ARLCB-TR-84033 SBI-AD-E440 261 F/G 6/4 NL

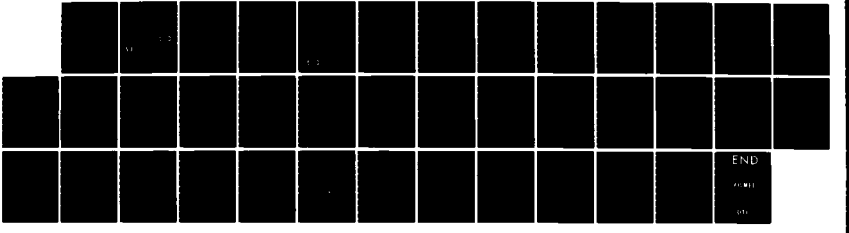

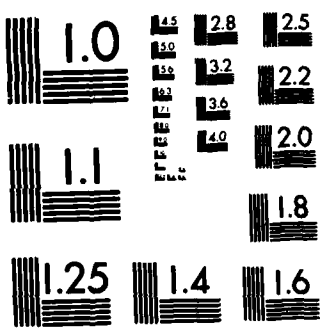

12

TECHNICAL REPORT ARLCB-TR-84033

AUTONOMOUS NAVIGATION FOR MOBILE ROBOT VEHICLES OVER HILLY TERRAIN USING RANGEFINDING MEASUREMENTS

C. N. SHEN

OCTOBER 1984

US ARMY ARMAMENT RESEARCH AND DEVELOPMENT CENTER
LARGE CALIBER WEAPON SYSTEMS LABORATORY
BENET WEAPONS LABORATORY
WATERVLIET N.Y. 12189

DISCLAIMER

The findings in this report are not to be construed as an official Department of the Army position unless so designated by other authorized documents.

The use of trade name(s) and/or manufacture(s) does not constitute an official indorsement or approval.

DISPOSITION

Destroy this report when it is no longer needed. Do not return it to the originator.

SECURITY CLASSIFICATION OF THIS PAGE (When Data Entered)

REPORT DOCUMENTATION PAGE		READ INSTRUCTIONS BEFORE COMPLETING FORM
1. REPORT NUMBER ARLCB-TR-84033	2. GOVT ACCESSION NO. AD-A148787	3. RECIPIENT'S CATALOG NUMBER
4. TITLE (and Subtitle) AUTONOMOUS NAVIGATION FOR MOBILE ROBOT VEHICLES OVER HILLY TERRAIN USING RANGEFINDING MEASUREMENTS		5. TYPE OF REPORT & PERIOD COVERED Final 6. PERFORMING ORG. REPORT NUMBER
7. AUTHOR(s) C. N. Shen		8. CONTRACT OR GRANT NUMBER(s)
9. PERFORMING ORGANIZATION NAME AND ADDRESS US Army Armament Research & Development Center Benet Weapons Laboratory, SMCAR-LCB-TL Watervliet, NY 12189		10. PROGRAM ELEMENT, PROJECT, TASK AREA & WORK UNIT NUMBERS AMCMS NO. 6111.02.H600.011 PRON NO. 1A325B541A1A
11. CONTROLLING OFFICE NAME AND ADDRESS US Army Armament Research & Development Center Large Caliber Weapon Systems Laboratory Dover, NJ 07801		12. REPORT DATE October 1984 13. NUMBER OF PAGES 32
14. MONITORING AGENCY NAME & ADDRESS(if different from Controlling Office)		15. SECURITY CLASS. (of this report) Unclassified 15a. DECLASSIFICATION/DOWNGRADING SCHEDULE

16. DISTRIBUTION STATEMENT (of this Report)

Approved for Public release, Distribution Unlimited.

17. DISTRIBUTION STATEMENT (of the abstract entered in Block 20, if different from Report)

18. SUPPLEMENTARY NOTES Presented at the Robotic Lntelligence & Productivity Conference, Wayne State University, Detroit Michigan, 18-19 Nov. 1983.

19. KEY WORDS (Continue on reverse side if necessary and identify by block number)

Mobile Robot
Vehicle Navigation
Obstacle Detection
Slope Estimation
Path Selection

20. ABSTRACT (Continue on reverse side if necessary and identify by block number)

The mobile robot vehicle is equipped with data acquisition and decision making devices for its autonomous navigation over rough terrain. A laser rangefinder is chosen as principal sensing device, which can determine radial distances from the vehicle to points on unpredictable hilly terrain surfaces. The overall procedure conducted for such a design consists of the following interrelated subsystems such as scanning scheme, obstacle detection scheme, terrain slope estimation, and path selection algorithm. Stochastic processes and methods are employed throughout the analysis.

DD FORM 1 JAN 73 1473 EDITION OF 1 NOV 65 IS OBSOLETE UNCLASSIFIED

SECURITY CLASSIFICATION OF THIS PAGE (When Data Entered)

TABLE OF CONTENTS

Page

TABLES

LIST OF ILLUSTRATIONS

INTRODUCTION

The successful development of an autonomous vision system for mobile robot vehicles would be of considerable value and importance to defense and related fields. Numerous reports and studies currently recommend artificial intelligence/robotics applications which require autonomous vehicles. Essential to these robotic vehicles is an adequate and efficient computer vision system. A potentially more successful approach, other than TV pictures and photographs, would be to develop a 3-D system employing a laser rangefinder. The author has been conducting studies for many years on application of a laser rangefinder vision system for a Mars autonomous rover vehicle. It seems feasible to transfer part of the technology and experiences obtained from the past Mars project to the present task on autonomous navigation for mobile robot vehicle over hilly terrains.

The scanning scheme takes into consideration the following: To detect the edges of an obstacle, the horizontal data spacing should be sufficiently small. From the viewpoint of estimation of the terrain slope, the possible spurious errors due to differentiation of the range data should be filtered. Outlines of obstacles on terrain surfaces are determined as discrete inputs to the system and the Rapid Estimation Scheme is utilized to detect the outlines of the obstacles. Smoothed estimates of range slopes are obtained by fitting a two-dimensional approximating function stochastically to a finite set of noise corrupted data from measuring the rough terrain. The in-path and cross-path terrain slopes and their variances at the data points are estimated from the set of corresponding range slopes. The path selection scheme is a decision-making process: A modified vector space algorithm is developed to

evaluate the corridor costs for a two-level radial corridor structure. Starting with the in-path slopes, cross-path slopes, obstruction height, and wheel deviation at the spine and track points, the algorithm is applied repeatedly to give a cost index to each corridor. An optimal path which minimizes the cost index is then determined using dynamic programming on the corridor structure.

THE NAVIGATION SYSTEM

A range matrix describing a certain scanned area of the terrain in front of the mobile robot, as shown in Figure 1, can be used to detect edges of discrete objects or to estimate the slopes of the terrain. With reference to the diagram in Figure 2, the Rapid Estimation Scheme was developed to process the range matrix and to detect the possible edges of obstacles. These detected points are fed into an obstacle identification scheme in which a whole set of detected points are classified into subsets. Each subset is recognized either as a boulder, a crater, or a hill. Then the locations and the sizes of the obstacles are used to determine the lengths of the passible corridors for the mobile robot vehicle. In parallel with the above procedures, the in-path and cross-path slopes of the terrain are estimated by a slope estimation scheme. These slope informations along the passible corridors are utilized to determine a safer and more accurate path for the mobile robot vehicle to travel.

The mobile robot vehicle is equipped with data acquisition and decision making devices for its autonomous navigation over rough terrain. A laser rangefinder is chosen as a principal sensing device, which can determine the

radial distances to the unpredictable hilly terrain surfaces. A rangefinder can be operated by emitting laser pulses and measuring the time of flight of a pulse between the instant it was transmitted and the instant the reflected pulse is received. This time of flight is related to the distance between the transmitter and the point on the terrain from which the pulse is reflected. With reference to Figure 1, the terrain is scanned by changing the azimuth (θ_j) and elevation (β_i) angles of the laser beam in a discrete fashion. The measurements are then available in the form of a NXM 'range-matrix' as follows:

$$M = [m_{i,j}],\ i=1,\ldots N;\ j=1,\ldots M \tag{1}$$

where each entry is modeled as:

$$m_{i,j} = \ell_{i,j} + v_{i,j} \tag{2}$$

where $\ell_{i,j}$ is the true range corresponding to the position angle (β_i, θ_j), and $v_{i,j}$ is a zero mean Gaussian noise sequence.

SCANNING SCHEME

The scanning scheme (ref 1) makes the compromise of two conflicting factors between that of not missing any sizeable obstacles, and that of accurately determining the gradient of the terrain. With reference to Figure 1, a rangefinder is located about 2 m above the ground. For navigation purposes, it is desired to cover a horizontal terrain from 5 m to 50 m in radial directions. The resolution of a rangefinder is limited by noise

---

[1]C. N. Shen and C. S. Kim, "A Laser Rangefinder Path Selection System for Martian Rover Using Logarithmic Scanning Scheme," VIII IFAC Symposium on Automatic Control in Space, Oxford, U.K., July 1979.

elements in positioning angles as well as the range error. It is assumed that the standard deviation of the positioning angles and the measured ranges are σ_β = 1 arc minute and σ_m = 0.05 m, respectively.

(i) The incremental pointing angle $\Delta\beta$ should be greater than its standard deviation, i.e., $\Delta\beta > \sigma_{\Delta\beta} = \sqrt{2}$ arc minute.

(ii) From the viewpoint of the obstacle detection scheme, the scheme needs at least three data points on the face of the obstacles. Thus, to detect the edges of an obstacle whose dimension is greater than 2 m in size, the horizontal data spacing $\Delta\rho$ should be less than (2/3)m.

(iii) From the viewpoint of the slope estimation of the terrain, it is necessary to consider the possible spurious errors in the slope estimation due to range errors where σ_m = 0.05 m.

Figure 3 indicates a possible spurious error in the estimated slope for a flat terrain. If $m_{i,j} = \ell_{i,j} - \sigma_m$ and $m_{i+1,j} = \ell_{i+1,j} + \sigma_m$, the resultant erroneous slope would be (σ_y/σ_x) instead of zero. Thus, we call (σ_y/σ_x) as a slope error index. In the previous research it was reported that this index is a function of the elevation angle $\beta_{i,j}$:

$$\gamma(\beta_i,\Delta\beta) = \sigma_y/\sigma_x = 2\sigma_m \sin\beta\{h[(\Delta\beta/\sin^2\beta) - 2\sigma_m \cos\beta]\}^{-1} \quad (3)$$

where

$$\beta = (\beta_i + \beta_{i+1})/2 \quad (3a)$$

$$\Delta\beta = \beta_{i+1} - \beta_i \quad (3b)$$

With reference to the design criteria (ii) and (iii) above, one would like to have a scanning scheme which satisfies the constraints; $\Delta\rho \leq (2/3)m$, and $\gamma \leq 0.25$. It is noted that these are two conflicting factors. It is concluded that the use of a constant $\Delta\beta$ for the whole region is prohibitive.

Therefore, it is proposed to divide the whole area into three sub-areas, and use different β for each. Table I shows a set of $\Delta\beta$'s for three sub-areas. Area 1 is close by, while area 3 is far away.

TABLE I. SCANNING SCHEME (ALL ANGLES IN RADIANS)

	β_{max}	β_{min}	$\Delta\beta$	$\Delta\theta$
Area 1	0.5039	0.1937	0.0282	0.03
Area 2	0.3115	0.117	0.0083	0.03
Area 3	0.15058	0.03590	0.00217	0.03

For this scanning scheme, the resultant horizontal data spacing $\Delta\rho$ and the slope error induces γ are shown in Figure 4. Here, it is noted that the proposed scanning scheme satisfies the constraints $\gamma < 0.25$ and $\Delta\rho < (2/3)m$ except that $\Delta\rho > (2/3)m$ for $\rho > 25$ m. However, this is justifiable in that, at far distances, we do not require as good a resolution as the one at near distances.

OBSTACLE DETECTION

Detection of Discrete Obstacles

Rapid Estimation Scheme (refs 2,3) has been developed to estimate and detect the discrete inputs with unknown magnitude which occur at unknown instances of time. Outlines of obstacles are considered as discrete changes

---

[2]R. V. Sonalker and C. N. Shen, "Mars Obstacle Detection by Rapid Estimation Scheme From Noisy Laser Rangefinder Readings," Proceedings of the Milwaukee Symposium on Automatic Computation and Control, Wisconsin, April 1975, pp. 291-296.

[3]C. S. Kim, R. C. Marynowski, and C. N. Shen, "Obstacle Detection Using Stabilized Rapid Estimation Scheme With Modified Decision Tree," Proceedings of JACC, Philadelphia, PA, October 1978.

in the slopes of the terrain. These discrete jumps are modeled as discrete inputs to the system and the R.E.S. is utilized to detect the outlines of the obstacles.

With reference to Figure 3, ℓ_i is the distance from the rangefinder to a point in the terrain and g_i is the incremental change in the adjacent ranges with constant azimuth angle. As is noticed, there occur sudden changes in g_i's both at the top and at the bottom of the boulder. This sudden change in g_i's is modeled as a discrete input u_k to the system as follows:

$$\begin{bmatrix} \ell_{i+1} \\ g_{i+1} \end{bmatrix} = \begin{bmatrix} \nu_i & 1-\mu \\ 0 & \zeta'_i \end{bmatrix} \begin{bmatrix} \ell_i \\ g_i \end{bmatrix} + \begin{bmatrix} \omega_i{}^1 \\ \omega_i{}^2 \end{bmatrix} + \begin{bmatrix} 0 \\ 1 \end{bmatrix} u_k \delta_{ik} \tag{4}$$

where $\omega_i{}^1$ and $\omega_i{}^2$ are plant noises and

$$\zeta'_i = (1-\Delta\beta_i \cdot \tan\ \beta_i)/(1+2\Delta\beta_i \cdot \cos\ \beta_i) \tag{5}$$

and

μ is a stabilizing factor $0 < \mu < 1$

and

$$\nu_i = 1-\mu(1-\xi_i) \tag{6}$$

where

$$\xi_i = (1+\Delta\beta_i \cdot \tan\ \beta_i)^{-1} \tag{7}$$

The corresponding measurement equation is:

$$m_{i+1} = \ell_{i+1} + v_{i+1} \tag{8}$$

where v_{i+1} is the measurement noise. At stage i, R.E.S. utilizes Kalman filter and input estimation scheme to estimate the states $[\ell_{i+1}, g_{i+1}]$, $[\ell_{i+2}, g_{i+2}]$, $[\ell_{i+3}, g_{i+3}]$, and $[\ell_{i+4}, g_{i+4}]$ under three different hypotheses:

H_1: an input exists between stages i and i+1.

H_2: an input exists between stages i+1 and i+2.

H_0: no input exists between stages i and i+2.

The joint conditional probability for each hypothesis is computed from the conditional state estimates and the measurement data. By using joint conditional probability, the hypothesis with minimum Bayes risk is accepted as a true hypothesis. Acceptance of H_1 as true hypothesis corresponds to a detection of an edge. If H_2 or H_0 is accepted, the scheme proceeds to the next stage. R.E.S. processes the range matrix, column-wise, to detect the vertical edges of the obstacles. It should be noted that single detection occurs at the bottom of the boulder or at the far edge of the crater. On the other hand, two consecutive detections occur at the top of the boulder or at the near edge of the crater. Side edges of the obstacles are detected by processing the range matrix row-wise.

Edge Detection Results

The simulation of terrain with hills and valleys is given in Figure 5. Figure 6 shows the edges of boulders, craters, and ridges detected by the rapid estimation scheme. The *'s and 0's indicate the edges detected by processing the range matrix column-wise and row-wise, respectively. The rapid estimation scheme also produces some false detections. Therefore, these detected edges are processed by a heuristic algorithm which classifies all the detected points as belonging to a boulder, crater, ridge, or false detections. Figure 7 shows the result of this obstacle identification scheme. Here, the characters 'B', 'C', and 'R' represent the edges of boulders, craters, and ridges, respectively. The three ridges shown at the top of Figure 7 are the

tops of the hills of which the centers are at (x,y) = (0,40), (-20,60), and (20,60) in Figure 5.

SLOPE ESTIMATION

Range Slopes Estimation

The slope estimation problem (refs 4,5) dealt with in this section is that of obtaining smoothed estimates of function values and particularly their derivatives from a finite set of inaccurate measurements in two-dimensions. In one approach we can identify the dynamic equations of the underlying system, or estimate the distributions for the quantities of interest and then apply optimal estimation algorithms. In some engineering problems the stochastic system may not be identified easily and in these situations, spline smoothing has proved to be a useful alternative.

In this report, we obtain the smoothed estimates of the slopes by utilizing a two-dimensional smoothing algorithm. For the problem of smoothing a finite set of noise corrupted data of an unknown function $f(\xi,\eta)$, it is proposed to obtain the smoothed estimate of $f(\xi,\eta)$ by fitting a two-dimensional approximating function $s(\xi,\eta)$ to the data set. For a set of measurements $m_{i,j}$ corrupted by a white noise process $v_{i,j}$:

$$m_{i,j} = f(\xi_i,\eta_i) + v_{i,j}, \quad \begin{matrix} i = 1,2,\ldots,N \\ j = 1,2,\ldots,M \end{matrix} \tag{9}$$

---

[4]C. S. Kim and C. N. Shen, "Design of a Recursive Vector Processor Using Polynomial Splines," Proceedings of the 19th IEEE Conference on Decision and Control, Albuquerque, NM, December 1980.

[5]C. S. Kim and C. N. Shen, "A Recursive Algorithm for Smoothing by Spline Functions," Proceedings of the International Congress on Applied Systems Research and Cybernetics, Acapulco, Mexico, December 1980.

an unknown function $f(\xi,\eta)$ is defined in the region $\{(\xi,\eta)\,|\,\xi_1 \leq \xi \leq \xi_N, \eta_1 \leq \eta \leq \eta_M\}$ is approximated by $s(\xi,\eta)$ which minimizes the following objective function:

$$J = \sum_{j=1}^{M} \sum_{i=1}^{N} [s(\xi_i,\eta_j) - m_{i,j}]^T R^{-1}_{i,j} [s(\xi_i,\eta_j) - m_{i,j}]$$

$$+ \rho \sum_{j=1}^{M-1} \sum_{i=1}^{N-1} \int_{\eta_j}^{\eta_{j+1}} \int_{\xi_i}^{\xi_{i+1}} z(\xi,\eta) d\xi d\eta \qquad (10)$$

where $\rho > 0$ is the smoothing parameter, $R_{i,j}$ is the observation error variance, $R_{i,j} \overset{\Delta}{=} E\{v_{i,j} \cdot v_{i,j}^T\}$, and $z(\xi,\eta)$ is some smoothness measure of $s(\xi,\eta)$ at (ξ,η).

Terrain Slopes and Range Slopes

With reference to Figure 1, terrain in-path and cross-path slopes are defined as the two orthogonal slopes $dz/d\rho$ and $dz/\rho d\theta$ in a cylindrical coordinate system. During the past investigations, the terrain slopes were found to be appropriate measures for evaluating a terrain. A direct approach for estimating the terrain slopes would be to fit a smoothing spline to the measurement data in cylindrical coordinates. However, there is a major difficulty in this approach: Even though the two independent variables β_i and θ_j for the rangefinder are changing with constant increments $\Delta\beta$ and $\Delta\theta$, respectively, the independent variable ρ_i in a cylindrical coordinate changes irregularly.

The recursive smoothing algorithm in the previous subsection requires that the data points be located at the corners of rectangular grids of the two independent variables. Since the two independent variables ρ_i and θ_j in a cylindrical coordinate system do not form rectangular grids, the smoothing

algorithm cannot be applied directly. By noting that the positioning angles β_i and θ_j are changing in regular fashion, it is proposed to obtain the smoothed estimates of the range slopes $dr/d\beta$ and $dr/d\theta$ defined in spherical coordinates. Then, these estimates are transformed to the terrain slopes.

In applying the smoothing algorithm to terrain slope estimation one point to be mentioned is that the basic philosophy of the smoothing spline approach is to suppress the noise elements by fitting a smooth approximating function to a noise corrupted data set. Thus, when the function to be approximated has sharp changes in its values or derivatives, the smoothing algorithm will produce errors in the results by smoothing out these actual sharp changes. From the viewpoint of terrain slope estimation, such changes occur at the edges of a boulder, a crater, or a ridge on the terrain. Thus, it is proposed to detect these edges by using the rapid estimation scheme. Then, for the area which is free of discrete edges, the two-dimensional smoothing algorithm is utilized to estimate the slopes. The terrain slopes are estimated in the order (i) discrete edges are detected by using the rapid estimation scheme; (ii) for the area which is free of discrete edges, a two-dimensional smoothing algorithm is utilized to estimate the range slopes; (iii) estimated range slopes are transformed into terrain slopes.

Estimated Terrain In-Path Slope

The estimated terrain in-path slopes (ref 6) are displayed in terms of a slope map, Figure 8. Characters A,...G represent a particular range of the

---

[6]C. S. Kim and C. N. Shen, "Estimating Planetary Terrain Slopes From Range Measurements Using a Two-Dimensional Spline Smoothing Technique," Proceedings of the 8th Triannual World Congress, International Federation of Automatic Control, August 1981, Kyoto, Japan.

terrain in-path slopes increasing from A to G, at the corresponding location. U represents undefined slopes. In Figure 8, we note circular slope regions on the faces of sinusoidal hills and valleys. Also, along a radial direction, the estimated slopes are changing slowly from one region of slopes to another. The large empty spaces are due to the hidden regions at the back of boulders or hills where laser rays could not reach. The undefined gradient represented by 'U' occurs when the recursive algorithm cannot be applied due to sharp changes in ranges between adjacent measurement data. The estimated in-path terrain slope maps are used for the evaluation of the terrain in front of the mobile robot vehicle.

Terrain Cross-Path Slopes

In discussing the terrain cross-path slopes (ref 7), the data can be conveniently processed to generate smoothed in-path and cross-path range slopes recursively in spherical coordinate system due to the regularity of the elevation and azimuth angles. When we proceed to calculate the true terrain slopes on the base plane, the regularity of the data points are completely destroyed. For a fixed elevation angle β, the horizontal projection of the range data are not located at a fixed distance from the rover. It is desired to calculate the cross-path slope at point (β_i, θ_j). However, in general, $\rho_{i,j} \neq \rho_{i,j+1}$. Thus, the true cross-path slope is not along an arc connecting points $\rho_{i,j}$ and $\rho_{i,j+1}$.

Our algorithm to calculate the terrain cross-path slope can then be summarized as follows:

---

[7] C. N. Shen and Poueau Shen, "The Estimation of Terrain Cross-Path Slopes," Proceedings of the 11th Annual Pittsburgh International Conference on Modeling and Simulation, University of Pittsburgh, May 1980.

1. Obtain the range measurements.

2. Use the smoothing algorithm to calculate the range cross-path slope.

3. Obtain the terrain cross-path slope and its variance.

PATH SELECTION

The path selection scheme (ref 8) is a decision-making process with the goal in determining an optimal path for the mobile robot vehicle to navigate. The first part of this scheme consists of data-acquisition, obstacle detection, gradient estimation, and interpolation algorithms. From these algorithms, the in-path and cross-path slopes and their covariances at the spine and track points are obtained. Using this information, a series of variables describing the features of the terrain will be calculated.

Based on the terrain variables, we quantify the corridor variables, risks, and costs for the corridors on which the optimal path selection algorithm is applied.

1. The input data comprises only the in-path and cross-path slopes and their variances.

2. The terrain variables are corrupted by noise. To consider the uncertainty in the measurements, N standard deviations are added to each terrain variable. Then the terrain variables are normalized with respect to their threshold values respectively.

3. The modified vector space algorithm is developed and applied repeatedly in the evaluation of the corridor variables later on, also in

---

[8]Poueau Shen and C. N. Shen, "Modified Vector Space Algorithm Applied to Path Selection Scheme," Proceedings of the 11th Annual Pittsburgh International Conference on Modeling and Simulation, University of Pittsburgh, May 1980.

evaluation of risks and costs.

Evaluation of Terrain Variables

As mentioned in the Introduction, in the evaluation of terrain variables, we only use the slopes at the spine and track points. The reason is two-fold. First, only a minor part of this path selection scheme need the data of elevation, which can be generated by the slopes. Second, if we adopt the elevation estimates as our input data, we will get larger errors in the calculation of in-path and tilt slope terrain variables.

The expressions of the terrain variables and the variances together with the corresponding explanations are listed below:

$$I(k) = [s(1,1) + s(3,1) + s(1,3) + s(3,3)]/4$$

$$\sigma_I^2(k) = [\sigma_s^2(1,1) + \sigma_s^2(3,1) + \sigma_s^2(1,3) + \sigma_s^2(3,3)]/16 \qquad (11)$$

$$X(k) = [c(1,1) + c(3,1) + c(1,3) + c(3,3)]/4$$

$$\sigma_X^2 = [\sigma_c^2(1,1) + \sigma_c^2(3,1) + \sigma_c^2(1,3) + \sigma_c^2(3,3)]/16 \qquad (12)$$

$$B(k) = \text{MAX}\ (B_1, B_2, B_3, B_4, B_5, B_6)\ ,$$

$$\text{typical B's, e.g. } B_4 = \frac{b}{8}\,[c(3,1) - c(1,1)]$$

$$\sigma_B^2(k) = \sigma^2(k = \text{Index}(\text{MAX}(B))) \qquad (13)$$

$$W(k) = \frac{1}{2}\,|a(m_1-m_2) + b(n_1-n_2)|\ \cdot$$

$$m_1 = \frac{1}{2}\,[s(1,3) + s(1,1)]\ ,\quad m_2 = \frac{1}{2}\,[s(3,3) + s(3,1)]\ ,$$

$$n_1 = \frac{-1}{2}\,[c(1,1) + c(3,1)]\ ,\quad n_2 = \frac{-1}{2}\,[c(1,3) + c(3,3))]$$

$$\sigma_w^2(k) = \text{Var}(W(k)) \qquad (14)$$

where $s(\ell,m)$ and $c(\ell,m)$ are in-path and cross-path terrain slopes, respectively.

In-Path Terrain Variables. The in-path slope terrain variable I(k) gives the average of the in-path slopes for the four vehicle wheels at each section. This variable is a measure of the risk in the forward direction. The in-path slope terrain variable I(k) and its variance are expressed by Eq. (11).

Tilt Slope. Tilt slope terrain variable X(k) is used to estimate excessive cross-path slopes which may cause the vehicle to tip over. The tilt slope terrain variable and its variance are given by Eq. (12).

Obstruction Height. The obstruction height is calculated for six different locations at each discrete section of the terrain. The maximum value is then chosen as representative of this whole section.

In deriving the formula for a typical obstruction height, we use a third order polynomial to approximate the terrain elevation in each location. By differentiating this polynomial with respect to the distance, we get an expression for the slope. With the known data of slopes at the three points substituted into this expression, we can determine the coefficients of the polynomial. Using this polynomial, we can then find the obstruction height in this direction. The formula for obstruction height is given in Eq. (13).

Wheel Deviation. The wheel deviation variable W(k) describes the offset of any of the four wheels from a plane. Wheels on any three track points define a plane. For each combination of three wheels touching the terrain, the deviation of the fourth wheel with respect to this plane is defined as the wheel deviation. The formula is as shown in Eq. (14).

Normalization of Terrain Variables

The four terrain variables represent different characteristics of the terrain. They are normalized so that comparisons can be drawn from a common basis.

The normalization process of the terrain variables consists of two steps. First, N standard deviations are added to each variable to increase the reliability. Second, each variable is divided by its own threshold value, becoming non-dimensional and comparable. The formula and basic features of the normalization process are shown below.

$$I_N(k) = [I(k) + N\sigma_I(k)]/T_I$$

$$B_N(k) = [B(k) + N\sigma_B(k)]/T_B$$

$$X_N(k) = [X(k) + N\sigma_X(k)]/T_X$$

$$W_N(k) = [W(k) + N\sigma_W(k)]/T_W \qquad (15)$$

where the threshold values are

$$T_I = 0.51 = \tan 27^\circ \qquad T_B = 0.34 \text{ m}$$

$$T_X = 0.58 = \tan 30^\circ \qquad T_W = 0.8 \qquad (16)$$

a. Concerning the stochastic aspect of the data, we assume that the variables are Gaussian with standard deviation σ. As is noticed in Eq. (15), not only the mean value, but also the standard deviation of the estimated value is used for the computation of normalized terrain variables. The probability for the real quantity being less than the normalized terrain variable is 0.683 for N = 1 and 0.955 for N = 2, etc.

b. The second feature of the normalization is with respect to each threshold value. These threshold values represent the upper limit for the terrain variables in a sense that once they are exceeded, there will be

disaster or obstruction to the vehicle. By dividing each terrain variable by its threshold value, the terrain variables become non-dimensional and comparable.

Modified Vector Space Algorithm

Corridor variables are defined as the representative quantities for the terrain variables along a given corridor. They are evaluated by utilizing the terrain variables for discrete sections of each corridor as input. To emphasize the contribution of high-values of the terrain variables to a corridor, the Modified Vector Space Algorithm has been implemented. The formulas for the corridor variables U_C are as follows:

$$U_C = \left(\sum_{k=1}^{M} U_N^P(k)/M \right)^{1/P} \tag{17}$$

where $U_N(k)$ is the specific series of normalized terrain variable in concern. Equation (17) is basically a generalization of the norm of a vector space.

$$U = \text{Norm} = \left(\sum_{k=1}^{M} U_N^P(k) \right)^{1/P} \tag{18}$$

It should be noted that the modified norm is different from the usual norm in that it is divided by the number of elements M. The reason for this division is that our corridors may be of varied lengths (which means varied number of discrete sections). By doing this, corridors of different lengths can be compared.

There is an analogy between this algorithm and the logic gate for the case of $p = 1$ and $p = \infty$. The case of $p = 1$ corresponds to a multi-input AND gate, while $p = \infty$ corresponds to an OR gate.

In general, for the four terrain variables, we have the following formulas

$$I_c = \left(\sum_{k=1}^{M} I_N^P(k)/M \right)^{1/P}$$

$$B_c = \left(\sum_{k=1}^{M} B_N^P(k)/M \right)^{1/P}$$

$$X_c = \left(\sum_{k=1}^{M} X_N^P(k)/M \right)^{1/P}$$

$$W_c = \left(\sum_{k=1}^{M} W_N^P(k)/M \right)^{1/P} \qquad (19)$$

The risk index R, represents the overall effect of the four terrain variables.

Risk Index

Risk is defined as the overall contribution of the four corridor variables by the use of modified vector space algorithm.

$$R = [(I_c^P + X_c^P + B_c^P + W_c^P)/4]^{1/P} \qquad (20)$$

Radial Corridor Structure

In simulating the possible routes which the vehicle might take, a radial corridor structure is adopted. The structure consists of two levels, primary corridors and secondary corridors. The primary corridors represent the possible choice of paths, while the secondary corridors provide a preview of the farther terrain.

Short Length Penalty and Target Deviation Penalty

Short length penalty S and target deviation D are defined for each corridor as

$$S = \frac{\ell_T \cos \theta_T}{\ell \cos \theta} \qquad (21)$$

$$D = \sum_{i=1}^{m} \frac{\ell_n \sin \theta_n}{L_T} \tag{22}$$

where ℓ_n = 5 m: min corridor length

L_T = 25 m: threshold value of target deviation

θ_T = 45°: threshold value of azimuth angle

Subscript n refers to the n^{th} stage

Corridor Cost and Dynamic Programming

The corridor cost is due to the combined effect of risk, short length penalty, and target deviation penalty. The expression for the cost is as below:

$$C_{i,j} = [(R_{i,j}^P + S_{i,j}^P + D_{i,j}^P)/3]^{1/P} \tag{23}$$

where the subscripts represent the index of different levels of corridors and serve to distinguish the primary and secondary corridors.

After each corridor has been assigned a cost, dynamic programming is applied to determine the optimal path which minimizes the combined cost of two levels as expressed by the following formula

$$C_{optimal} = \underset{i}{\text{Minimize}} \{C_{i,0} + \underset{j}{\text{Minimize}}[C_{i,j}]\} \tag{24}$$

For a mathematical wavy terrain with obstacles superimposed, a computer simulation is performed to evaluate this path selection scheme.

CONCLUSIONS

A set of the measurement data is obtained by the described scanning scheme. Rapid estimation scheme detects the possible edges of the obstacles by processing the range measurement data. The points detected by this R.E.S. are identified either as a boulder, crater, ridge, or false detections. The

length of the corridors that a rover can travel is determined from the locations and sizes of the obstacles identified. Moreover, the range measurement data are processed by gradient estimation scheme to evaluate in-path and cross-path slopes at the data points. Since the slopes are estimated in the spherical coordinate system, it is needed to transform the range slope in spherical coordinate system to terrain slope in cylindrical coordinate.

The in-path and cross-path slopes and their covariances at the spine and track points along the corridors are evaluated by applying two-dimensional interpolation scheme over the estimated slopes at the data points. The terrain variables at a discrete section along each corridor are computed by using estimated slopes at the spine and track points. Since the terrain variable estimates have uncertainty, the present method increases the reliability by considering standard deviation as well as their mean values.

The path selection scheme evaluates risk index for each corridor by applying the modified vector space algorithm to the terrain variables. It is concluded that certain similarity exists between the autonomous navigation of the mobile robot vehicle and the Mars rover. The latter work can serve as a starting point for future research on navigation of mobile robot vehicle.

REFERENCES

1. C. N. Shen and C. S. Kim, "A Laser Rangefinder Path Selection System for Martian Rover Using Logarithmic Scanning Scheme," VIII IFAC Symposium on Automatic Control in Space, Oxford, U.K., July 1979.
2. R. V. Sonalker, and C. N. Shen, "Mars Obstacle Detection by Rapid Estimation Scheme From Noisy Laser Rangefinder Readings," Proceedings of the Milwaukee Symposium on Automatic Computation and Control, Wisconsin, April 1975, pp. 291-296.
3. C. S. Kim, R. C. Marynowski, and C. N. Shen, "Obstacle Detection Using Stabilized Rapid Estimation Scheme With Modified Decision Tree," Proceedings of JACC, Philadelphia, PA, October 1978.
4. C. S. Kim and C. N. Shen, "Design of a Recursive Vector Processor Using Polynomial Splines," Proceedings of the 19th IEEE Conference on Decision and Control, Albuquerque, NM, December 1980.
5. C. S. Kim and C. N. Shen, "A Recursive Algorithm for Smoothing by Spline Functions," Proceedings of the International Congress on Applied Systems Research and Cybernetics, Acapulco, Mexico, December 1980.
6. C. S. Kim and C. N. Shen, "Estimating Planetary Terrain Slopes From Range Measurements Using a Two-Dimensional Spline Smoothing Technique," Proceed-ings of the 8th Triannual World Congress, International Federation of Automatic Control, August 1981, Kyoto, Japan.
7. C. N. Shen and Poueau Shen, "The Estimation of Terrain Cross-Path Slopes," Proceedings of the 11th Annual Pittsburgh International Conference on Modeling and Simulation, University of Pittsburgh, May 1980.

8. Poueau Shen and C. N. Shen, "Modified Vector Space Algorithm Applied to Path Selection Scheme," Proceedings of the 11th Annual Pittsburgh International Conference on Modeling and Simulation, University of Pittsburgh, May 1980.

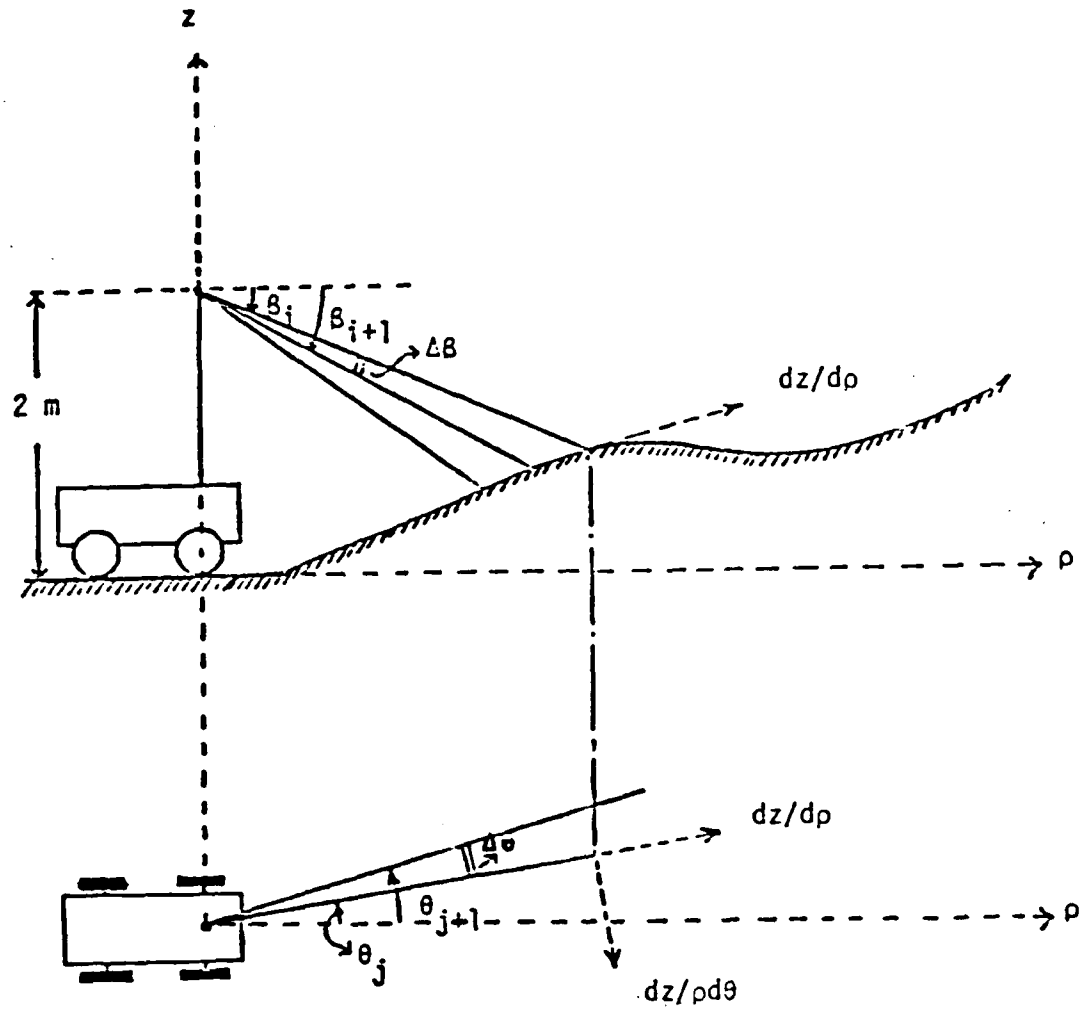

Figure 1. Top and side views of a rangefinder.

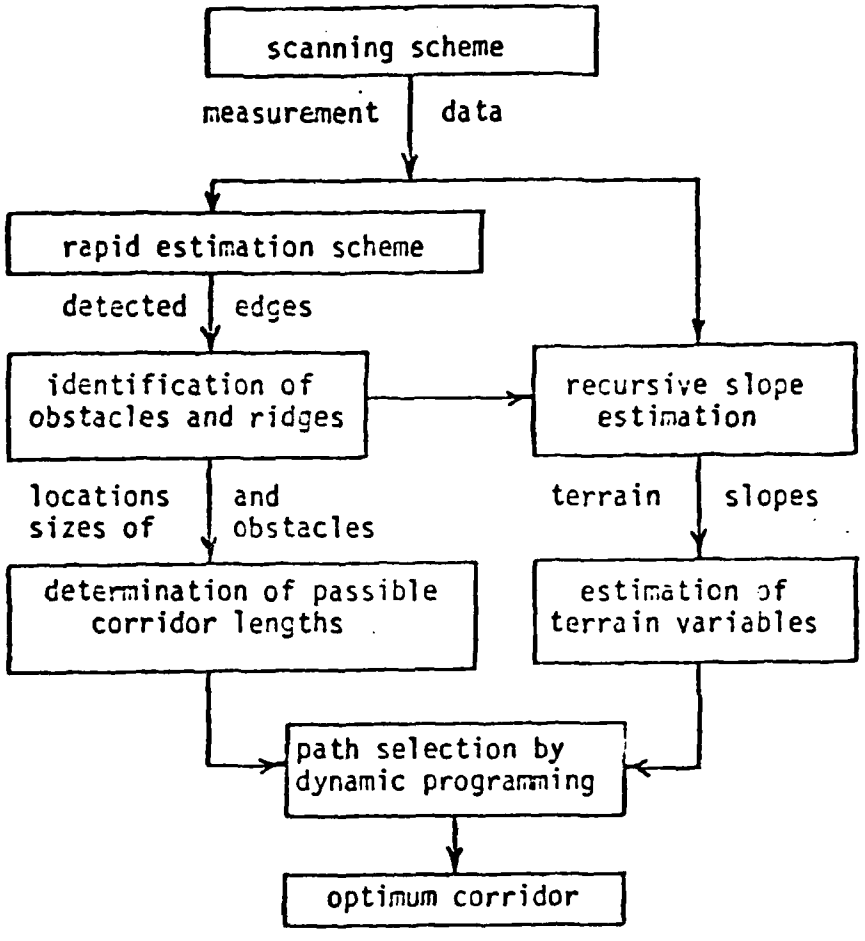

Figure 2. Flow diagram of the data acquisition and decision making system.

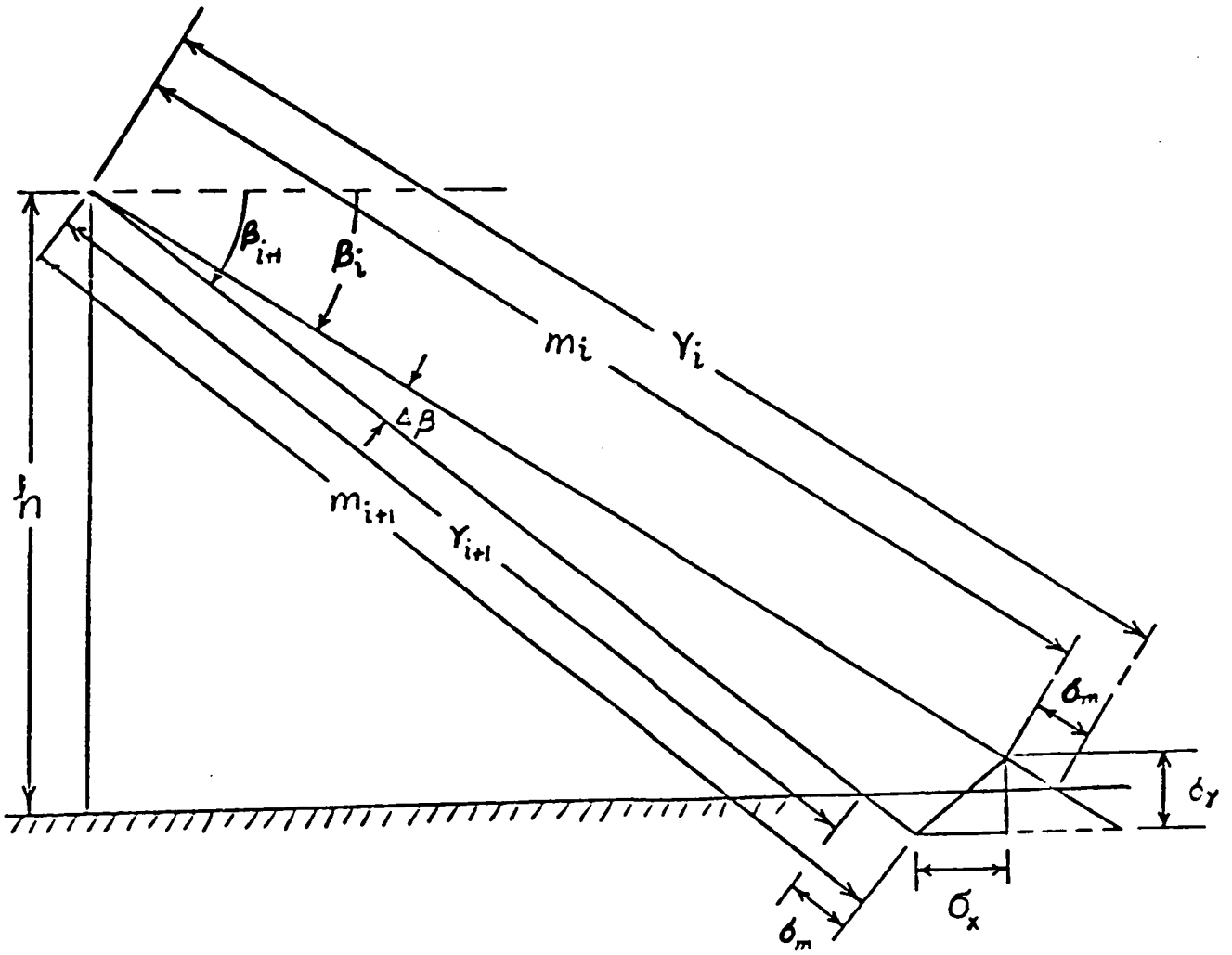

Figure 3. Error in slope estimation due to measurement noise.

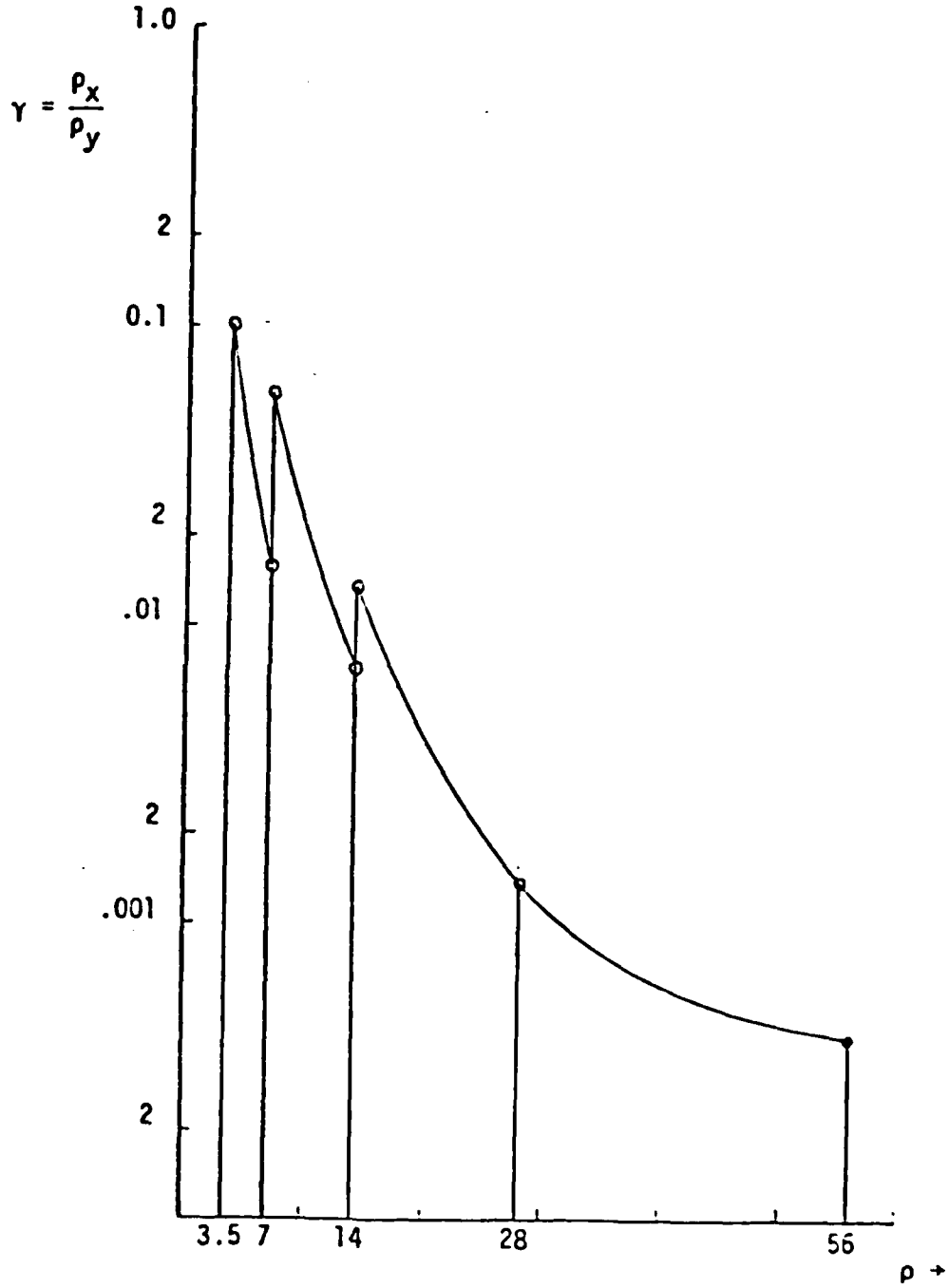

Figure 4a. Variation of slope error index with distance for the scanning scheme used.

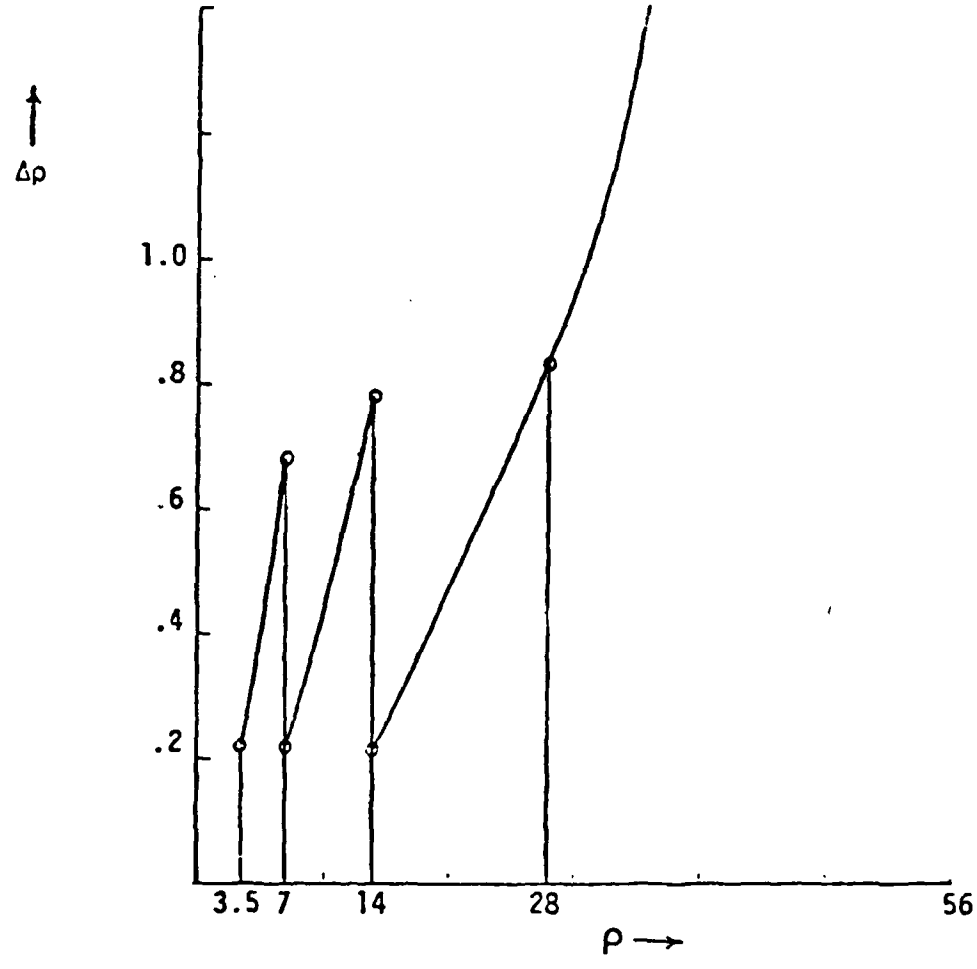

Figure 4b. Variation of horizontal spacing with distance for the scanning scheme used.

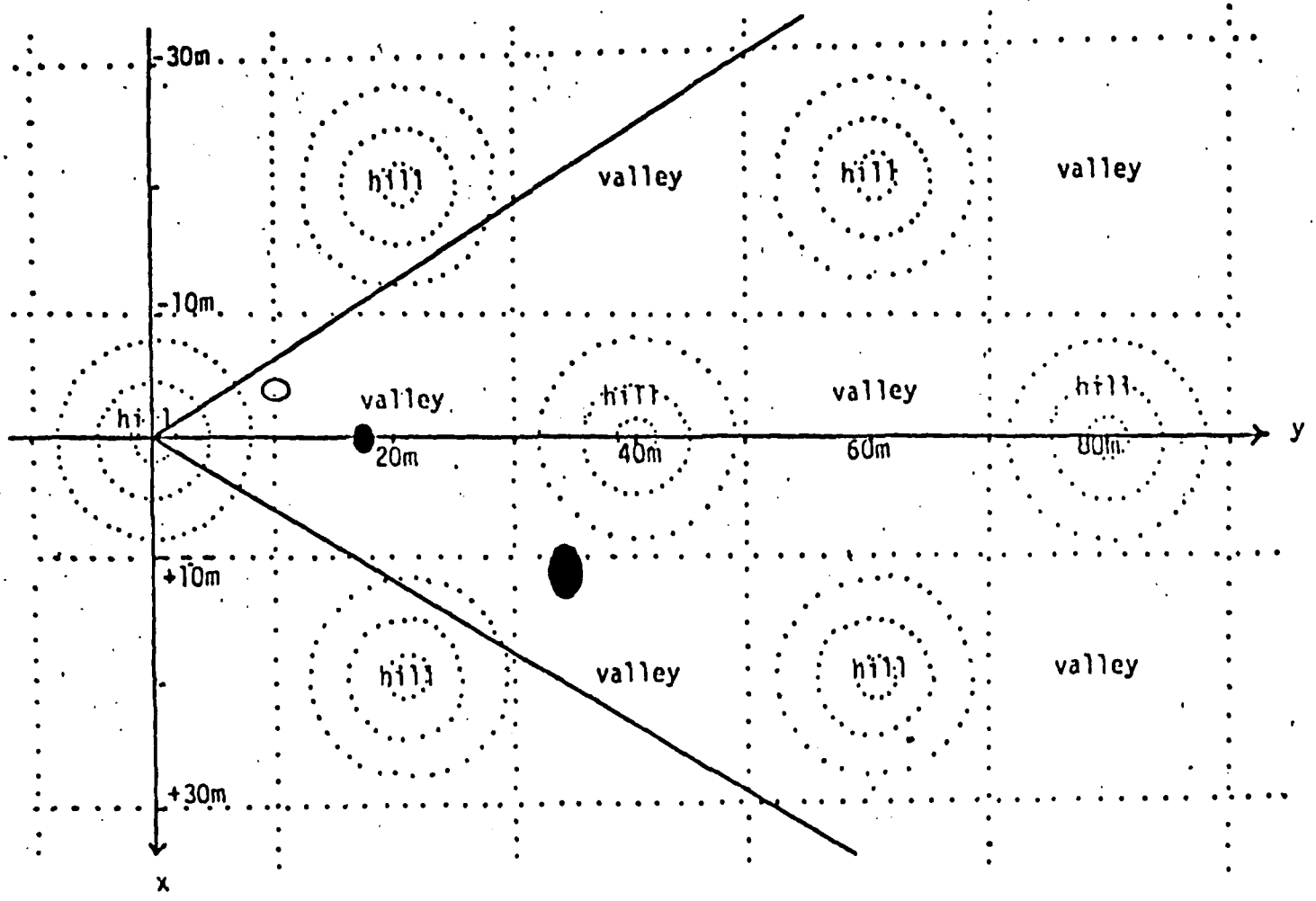

Figure 5. Top view of the terrain model used for simulation.

●.... boulder, , O.... crater

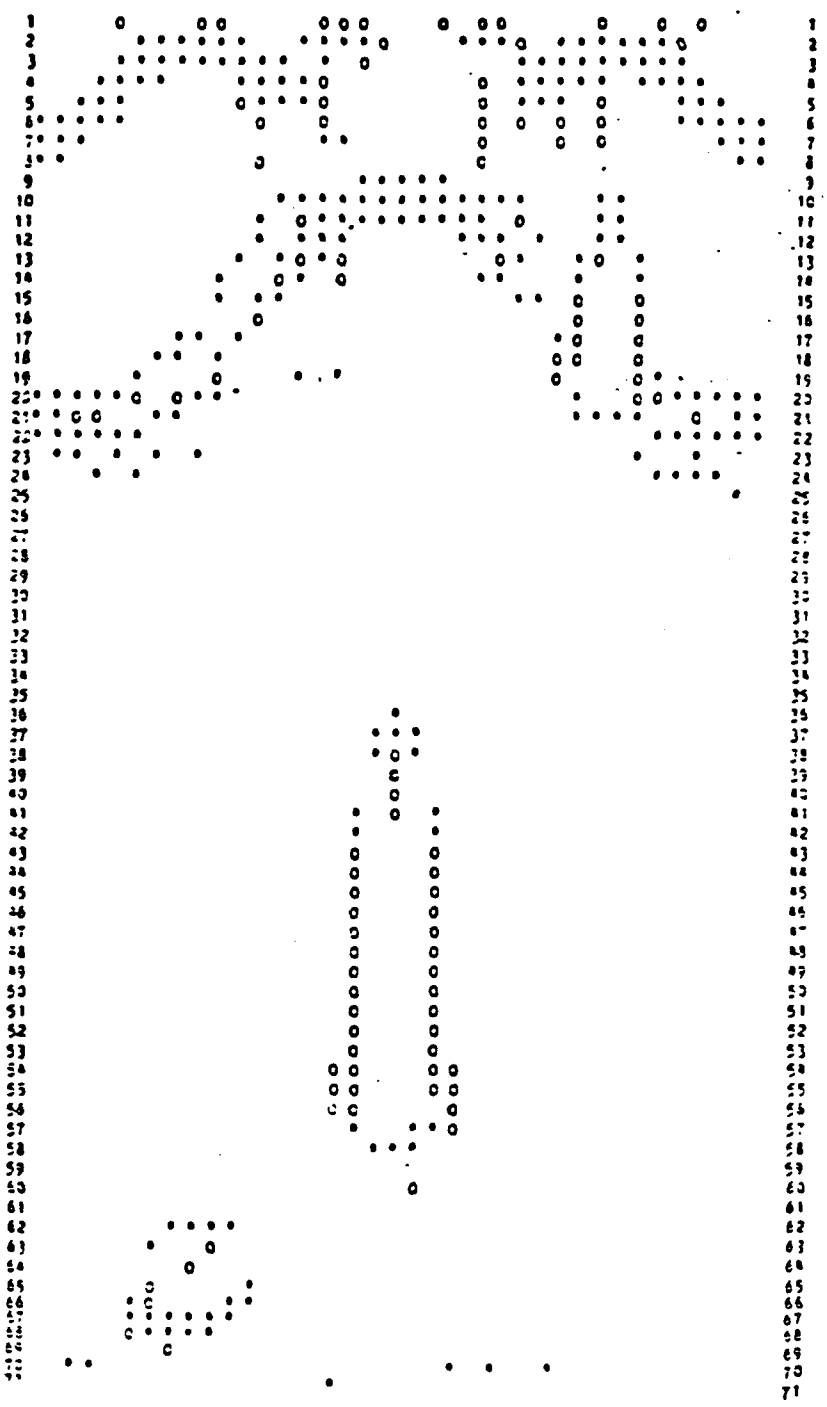

Figure 6. Detected edges of boulders, craters, and hills from rapid estimation scheme.

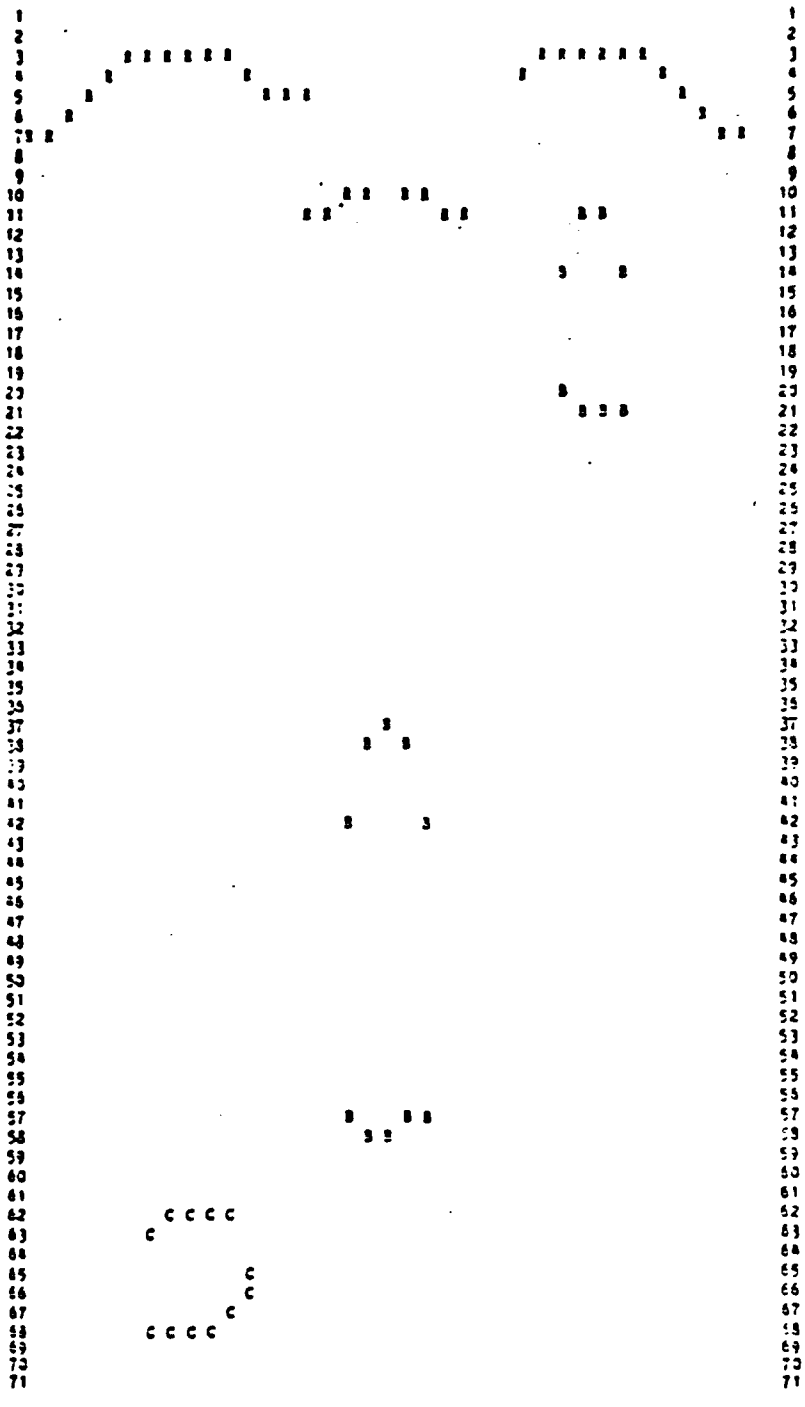

Figure 7. Outlines of boulders, craters, and hills.

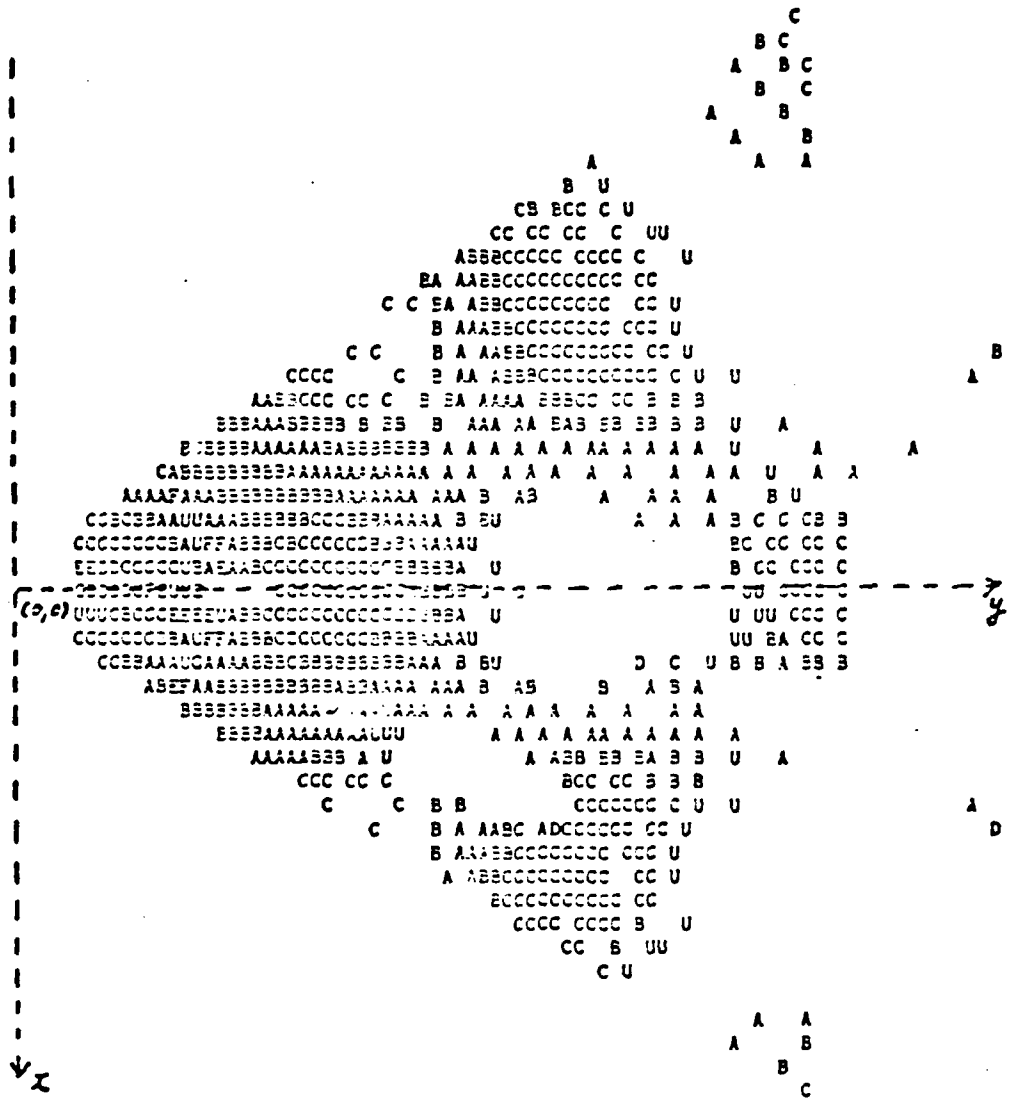

Figure 8. A slope map in the x-y plane for the in-path terrain slopes obtained from a two-dimensional smoothing algorithm.

TECHNICAL REPORT INTERNAL DISTRIBUTION LIST

	NO. OF COPIES
CHIEF, DEVELOPMENT ENGINEERING BRANCH	
ATTN: SMCAR-LCB-D	1
-DA	1
-DP	1
-DR	1
-DS (SYSTEMS)	1
-DS (ICAS GROUP)	1
-DC	1
CHIEF, ENGINEERING SUPPORT BRANCH	
ATTN: SMCAR-LCB-S	1
-SE	1
CHIEF, RESEARCH BRANCH	
ATTN: SMCAR-LCB-R	2
-R (ELLEN FOGARTY)	1
-RA	1
-RM	2
-RP	1
-RT	1
TECHNICAL LIBRARY	5
ATTN: SMCAR-LCB-TL	
TECHNICAL PUBLICATIONS & EDITING UNIT	2
ATTN: SMCAR-LCB-TL	
DIRECTOR, OPERATIONS DIRECTORATE	1
DIRECTOR, PROCUREMENT DIRECTORATE	1
DIRECTOR, PRODUCT ASSURANCE DIRECTORATE	1

NOTE: PLEASE NOTIFY DIRECTOR, BENET WEAPONS LABORATORY, ATTN: SMCAR-LCB-TL, OF ANY ADDRESS CHANGES.

TECHNICAL REPORT EXTERNAL DISTRIBUTION LIST

	NO. OF COPIES
ASST SEC OF THE ARMY RESEARCH & DEVELOPMENT ATTN: DEP FOR SCI & TECH THE PENTAGON WASHINGTON, D.C. 20315	1
COMMANDER DEFENSE TECHNICAL INFO CENTER ATTN: DTIC-DDA CAMERON STATION ALEXANDRIA, VA 22314	12
COMMANDER US ARMY MAT DEV & READ COMD ATTN: DRCDE-SG 5001 EISENHOWER AVE ALEXANDRIA, VA 22333	1
COMMANDER ARMAMENT RES & DEV CTR US ARMY AMCCOM ATTN: SMCAR-LC	1
SMCAR-LCE	1
SMCAR-LCM (BLDG 321)	1
SMCAR-LCS	1
SMCAR-LCU	1
SMCAR-LCW	1
SMCAR-SCM-O (PLASTICS TECH EVAL CTR, BLDG. 351N)	1
SMCAR-TSS (STINFO) DOVER, NJ 07801	2
DIRECTOR BALLISTICS RESEARCH LABORATORY ATTN: AMXBR-TSB-S (STINFO) ABERDEEN PROVING GROUND, MD 21005	1
MATERIEL SYSTEMS ANALYSIS ACTV ATTN: DRXSY-MP ABERDEEN PROVING GROUND, MD 21005	1
COMMANDER US ARMY AMCCOM ATTN: SMCAR-ESP-L ROCK ISLAND, IL 61299	1
COMMANDER ROCK ISLAND ARSENAL ATTN: SMCRI-ENM (MAT SCI DIV) ROCK ISLAND, IL 61299	1
DIRECTOR US ARMY INDUSTRIAL BASE ENG ACTV ATTN: DRXIB-M ROCK ISLAND, IL 61299	1
COMMANDER US ARMY TANK-AUTMV R&D COMD ATTN: TECH LIB - DRSTA-TSL WARREN, MI 48090	1
COMMANDER US ARMY TANK-AUTMV COMD ATTN: DRSTA-RC WARREN, MI 48090	1
COMMANDER US MILITARY ACADEMY ATTN: CHMN, MECH ENGR DEPT WEST POINT, NY 10996	1
US ARMY MISSILE COMD REDSTONE SCIENTIFIC INFO CTR ATTN: DOCUMENTS SECT, BLDG. 4484 REDSTONE ARSENAL, AL 35898	2
COMMANDER US ARMY FGN SCIENCE & TECH CTR ATTN: DRXST-SD 220 7TH STREET, N.E. CHARLOTTESVILLE, VA 22901	1

NOTE: PLEASE NOTIFY COMMANDER, ARMAMENT RESEARCH AND DEVELOPMENT CENTER, US ARMY AMCCOM, ATTN: BENET WEAPONS LABORATORY, SMCAR-LCB-TL, WATERVLIET, NY 12189, OF ANY ADDRESS CHANGES.

TECHNICAL REPORT EXTERNAL DISTRIBUTION LIST (CONT'D)

	NO. OF COPIES
COMMANDER US ARMY MATERIALS & MECHANICS RESEARCH CENTER ATTN: TECH LIB - DRXMR-PL WATERTOWN, MA 01272	2
COMMANDER US ARMY RESEARCH OFFICE ATTN: CHIEF, IPO P.O. BOX 12211 RESEARCH TRIANGLE PARK, NC 27709	1
COMMANDER US ARMY HARRY DIAMOND LAB ATTN: TECH LIB 2800 POWDER MILL ROAD ADELPHIA, MD 20783	1
COMMANDER NAVAL SURFACE WEAPONS CTR ATTN: TECHNICAL LIBRARY CODE X212 DAHLGREN, VA 22448	1
DIRECTOR US NAVAL RESEARCH LAB ATTN: DIR, MECH DIV	1
CODE 26-27, (DOC LIB) WASHINGTON, D.C. 20375	1
COMMANDER AIR FORCE ARMAMENT LABORATORY ATTN: AFATL/DLJ	1
AFATL/DLJG EGLIN AFB, FL 32542	1
METALS & CERAMICS INFO CTR BATTELLE COLUMBUS LAB 505 KING AVENUE COLUMBUS, OH 43201	1

NOTE: PLEASE NOTIFY COMMANDER, ARMAMENT RESEARCH AND DEVELOPMENT CENTER, US ARMY AMCCOM, ATTN: BENET WEAPONS LABORATORY, SMCAR-LCB-TL, WATERVLIET, NY 12189, OF ANY ADDRESS CHANGES.

END

FILMED

1-85

DTIC